The detailed integration is monitored continually and maximum dimensionalized values of the desired variables in $\mathbf{Y}(t)$ are displayed.

The solutions of the boundary value problems, Eqs. (11) and (12), result in mode shapes in which greatest deflection and curvature appear at the boom tip and root, respectively, for all cases studied. Some typical shapes are shown in Fig. 2 for the example described later.

The integration of Eq. (14) clearly shows the main body motion being slightly (except for despin) altered by the effects of extension and vibration of the boom. Moreover, in cases where the instantaneous transient natural frequency of vibration of the booms is much higher than the nutation—precession frequency, the results show a high frequency transient vibration of the booms being modulated by the low frequency inertial loading they experience.

A number of cases were analyzed by the program. One such case was a single dipole boom pair being symmetrically extended from a main body with a nonsymmetric inertia ellipsoid. The parameters used are as follows: $I_{11} = 14.2$ slug-ft^2; $I_{22} = 13.78$ slug-ft^2; $I_{33} = 15.09$ slug-ft^2; $EI_i = 1.735$ lb-ft^2; $\rho_i = 1.685 \times 10^{-4}$ slug/ft; $M_{ti} = 4.115 \times 10^{-4}$ slug; $l_i = 0.0417$ fps; $l_{i\text{final}} = 23.5$ ft; $b_i = 1.1$ ft; $h_i = 1.5$ ft; $\Psi_1 = 14°$; $\Psi_2 = 194°$

$$\text{Initial coning angle} \cong 1°$$

$$\dot{\alpha}_3(0) \cong 3.3 \text{ rad/sec}$$

The results appear in Table 1. A typical value for Ω_n, the nutation—precession frequency in ϕ, for this example varied between 0.075 and 0.1.

If Eqs. (7) and (8) are reduced to fourth-order partial differential equations without making the indicated simplifications in Eqs. (9) and (10), the general linearized partial differential equations of boom motion result. Another approach to the boom extension problem consists of solving these equations together with the equation for the conservation of the satellite angular momentum.

Several interesting effects are evident in the dynamics of a satellite with extending booms. For example, in-plane ($\mathbf{j}_2$) vibrations are influenced by despin and Coriolis forces as well as nutation. Out-of-plane ($\mathbf{j}_3$) vibrations are affected mainly by nutation. The "centrifugal stiffening" is greatest for out-of-plane vibrations. One result of such a combination of effects is that in-plane vibrations are nonsymmetric and can easily become greater than out-of-plane vibrations if the despin rate is high, as can be seen from Table 1.

Conclusions

The analysis and program developed are useful for determining the dynamics of satellites under deployment of long flexible booms and could be used to find the typical dynamics during normal operation after deployment. The program parameters are arbitrary within the confines of a spin-stabilized configuration and can be specified for each boom independently.

An example indicated that the satellite modelled should be left with a small "coning" angle after extension, and that its booms are not in danger of buckling. Increases in initial coning angle result in proportionate increases in maximum values. Thus, predictions for other initial coning angles can easily be made from Table 1 for the satellite modelled; this is to be expected, since the approximate equations of motion used are linear.

References

[1] Josloff, A. T., "Systems Constraints Imposed on Spacecraft Utilizing Long Extendible Rods with Attached Tip Masses," *AIAA/ASME 8th Structures, Structural Dynamics and Materials Conference*, AIAA, N. Y.

[2] Lang, W. E. and Honeycutt, G. N., "Simulation of Deployment Dynamics of Spinning Spacecraft," TN D-4074, Aug. 1967, NASA.

[3] Bowers, E. J. and Williams, C. E., "Optimization of RAE Satellite Boom Deployment Timing," *Journal of Spacecraft and Rockets*, Vol. 7, No. 9, Sept. 1970, pp. 1057–1062.

[4] Cloutier, G. J., "Dynamics of Deployment of Extendible Booms from Spinning Space Vehicles," *Journal of Spacecraft and Rockets*, Vol. 5, No. 5, May 1968, pp. 547–552.

[5] Hughes, P. C. and Cherchas, D. B., "Influence of Solar Radiation on the Spin Behaviour of a Satellite with Long Flexible Antennae," *CASI Transactions*, Vol. 2, No. 2, Sept. 1969, pp. 53–57.

Effects of Surface Roughness on Heat Transfer to Ablating Bodies

JIN H. CHIN*
Lockheed Missiles & Space Company, Sunnyvale, Calif.

Nomenclature

C_c = $(\rho_*/\rho_e)^{0.8}(\mu_*/\mu_e)^{0.2}$
k = roughness dimension
K_r = roughness correction factor
N = surface inward normal
R = roughness function
Re_k = roughness Reynolds Number $\rho_e u_e k/\mu_e$
Re_θ = momentum-thickness Reynolds Number $\rho_e u_e \theta/\mu_e$
St = zero-blowing Stanton Number
$\bar{St}$ = blowing Stanton Number
T = absolute Temperature
u = tangential velocity
μ = viscosity
ρ = density

Subscripts

c = between minimum and maximum values
e = at boundary layer edge
L = laminar boundary layer
T = turbulent boundary layer
r = rough surface
w = at wall conditions
$*$ = reference enthalpy conditions

Introduction

TO include the effects of surface roughness on thermal response predictions for ablating bodies, an adequate theory must be able to account for the following: 1) effects of surface roughness on heating and pressure distribution, and 2) characterization of roughness variation with time during the heating environment history. The effects of surface roughness on turbulent skin friction and heat transfer have been studies by a number of investigators.[1–4] Some results indicate that large surface roughness increases the stagnation-point heat transfer.[5,6] Other results show that roughness does not increase the heat transfer at the stagnation point nor at other parts of the body when the flow remains laminar.[7] For nonblowing, smooth walls the method of Persh[8] provides a reasonable correlation with experimental heating data in the transitional boundary layer regime.[9] The formation of cross-hatching generally requires a supersonic transitional or turbulent boundary layer.[10] Large variation in heating exposure time required for initiation of cross-hatching for different

Received July 13, 1970; revision received February 22, 1971. The work was performed with support from Contract F0-4701-68-C-0299.

* Staff Engineer, Aero-Thermodynamics Department, Engineering Technology. Member AIAA.

materials indicates that the pattern formation is a material response phenomenon.[10]

The purpose of this Note is to present a simple engineering calculation procedure which may be readily adapted to existing computer routines for smooth wall heating distributions.

Model

The model involves the following assumptions:

1) By definition, the beginning of the transitional region coincides with the first deviation from laminar flow predictions. The effect of surface roughness is negligible when the flow remains laminar.

2) The effects of roughness on nonblowing turbulent heating is correlated by a roughness correction factor K_r, a ratio of heat transfer coefficient with roughness to that for a smooth wall.

3) The Persh[8] method of transitional boundary layers for smooth walls is applicable for roughened surfaces.

4) The correlation of blowing effectiveness for smooth walls is applicable for roughened surfaces, i.e., $\bar{St}_r/St_r = \bar{St}/St$. The mass transfer effects for the transitional region is accounted for by an interpolation procedure.

5) Before the onset of transition, the surface roughness characteristic dimension is assumed to be at the minimum or initial value (e.g., material grain size). A convenient location is selected on the conical portion of the body to monitor the surface recession after the point of transition has passed over this point. The roughness dimension, considered uniform over the transitional and turbulent regions, is allowed to increase to a selected maximum value. After the monitored recession reaches this maximum value, no further increase in roughness size is considered.

Effects of roughness on nonblowing turbulent heating

Fenter[3] obtains an equation relating the momentum thickness to the local skin friction for compressible turbulent boundary layer on uniformly rough surfaces. This equation is derived from the law of the wall velocity profile and, therefore, is applicable to flows with pressure gradients. With a Reynolds analogy factor of unity and from Fenter's equation, the following expression for the roughness correction factor is readily obtained

$$K_r = \frac{St_{T,r}}{St_T} = \left\{1 - \left(\frac{R}{2^{1/2}}\right)\Big/\left[4.13\log_{10}\mathrm{Re}_\theta + 4.13\log_{10}\left(\frac{\mu_e}{\mu_w}\right) + 2.9\right]\right\}^{-2} \quad (1)$$

where $R = R(\eta_k)$ is a roughness function for incompressible flow in pipes with grain-type surface roughness.

$$\eta_k = (\mu_e/\mu_w)(T_e/T_w)^{1/2}Re_kSt_{T,r}^{1/2} \quad (2)$$

The function $R(\eta_k)$ may be approximated by

$$R_i(\eta_k) = a_i \ln\eta_k + b_i \quad (3)$$

The values of a_i and b_i are given in Table 1. For convenience of calculation, $St_{T,r}$ in Eq. (3) is evaluated at the previous body surface point.

As k increases, $K_r \to \infty$ when the two terms within the braces of Eq. (1) become equal. However, the Reynolds analogy is expected to break down before this limit is approached. The results of Dipprey and Sabersky[11] for incompressible flow inside nickel tubes indicate that surface roughness increases the Stanton number by a ratio of 2.7 (with even larger increase in skin-friction coefficient) of the smooth-wall value. The upper limit is likely dependent upon the roughness conductivity, geometry, and other parameters. Here an upper limit ratio of 3.0 is assumed.

Table 1 Roughness function constant

Zone	i	η_k	a_i	b_i
Smooth	1	$\eta_k \leq 5$	0	0
Transitional	2	$5 < \eta_k \leq 100$	2.84	−4.58
Fully rough	3	$100 < \eta_k$	2.50	−3.00

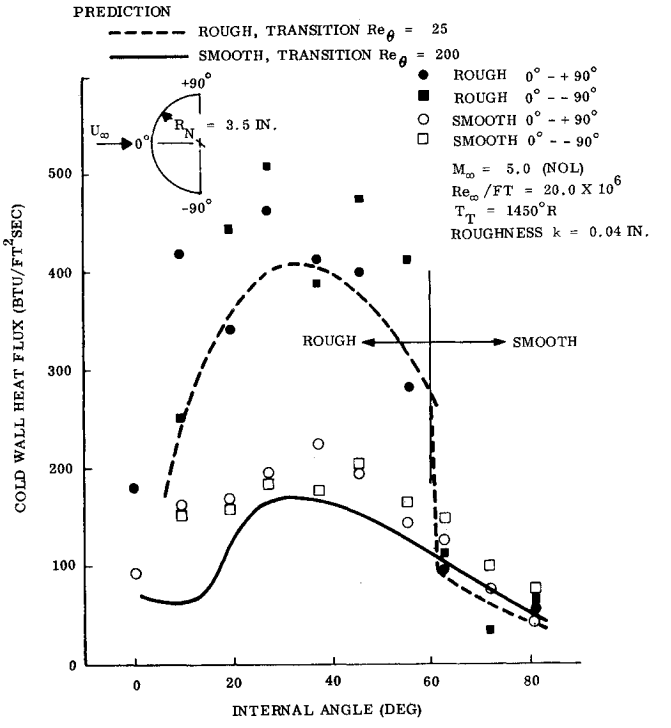

Fig. 1 Heat transfer on smooth and rough hemispheres.

Transitional heating on rough surfaces

The modified Persh equation may be written as

$$St_r = K_rSt_T - \alpha/Re_\theta^2 \quad (4)$$

The value of the constant α is determined by requiring a continuity of St and Re_θ at the point of transition onset. The value of Re_θ is computed by integration of the momentum integral equation invoking local similarity with entropy layer swallowing effects. The smooth-wall tubulent heat transfer is calculated by

$$St_T = 0.0126C_e^{1.25}Re_\theta^{-0.25} \quad (5)$$

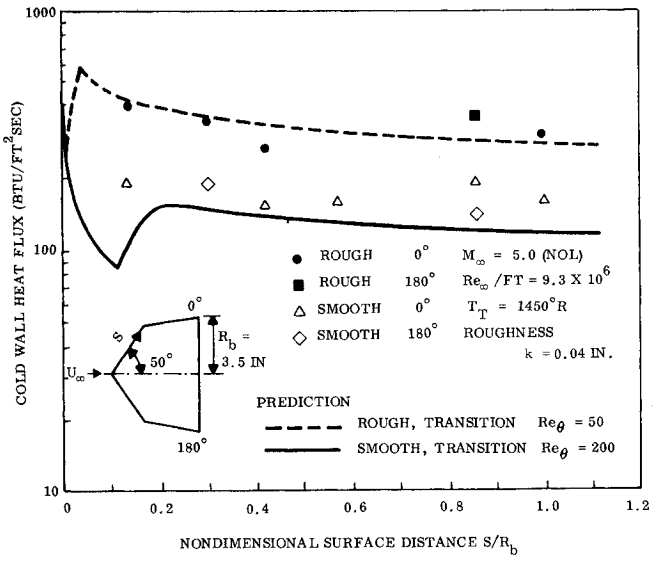

Fig. 2 Heat transfer on smooth and rough cones.

The mass transfer parameter and recovery factor are calculated by interpolation between the laminar and turbulent values in terms of the factor

$$F = \log_{10}(St_r/St_L)/\log_{10}(K_r St_T/St_L) \quad (6)$$

The transitional heating regime corresponds to $0 < F < 0.99$.

Growth of Monitored Surface Roughness

Between the initial and the maximum roughness dimensions [assumption (5)], the surface-roughness growth rate may be expressed as a function of pressure, Reynolds number, surface roughness, surface recession rate, and other variables:

$$dk/dt = f(p,Re,k,dN/dt, \ldots) \quad (7)$$

Before the functional form is determined by extensive theoretical and experimental studies, the following relationship may be considered ($n > 1$):

$$\frac{dk}{dt} = \begin{cases} [(k - k_{\min})/(k_c - k_{\min})]^{1/n}(dN/dt), & k_{\min} < k \leq k_c \\ [(k_{\max} - k)/(k_{\max} - k_c)]^{1/n}(dN/dt), & k_c < k < k_{\max} \end{cases} \quad (8)$$

Integration of Eq. (8) between limits $k_{\min}$ and $k_{\max}$ yields

$$\Delta N = [n/(n - 1)](k_{\max} - k_{\min}) \quad (9)$$

The case $n \to \infty$ corresponds to the upperlimit roughness growth rate, provided no surface fracture occurs. On the other hand, zero growth rate corresponds to $n = 1$.

Application of Methods

The present method is used to predict the heat-transfer rate on roughened hemispheres and cones presented recently by Thyson et al.[12] Reasonable agreements between prediction and data are obtained, as shown in Figs. 1 and 2.

Experimental data have not been found to validate the assumption on surface roughness growth. Nevertheless, Eqs. (8) and (9) may be used in parametric sensitivity studies, particularly when an approximate estimate of the magnitude of recessions is available.

References

[1] Schlichting, H., *Boundary Layer Theory*, 4th ed., McGraw-Hill, New York, 1960, pp. 457–565.

[2] Welsh, W. E., Jr., "Shape and Surface Roughness Effects on Turbulent Nose Tip Ablation," AIAA Paper 69-717, San Francisco, Calif., 1969.

[3] Fenten, F. W., "The Turbulent Boundary Layer on Uniformly Rough Surfaces at Supersonic Speeds," Rept. DRL-437, Jan. 1960, Defense Research Lab., The Univ. of Texas, Austin, Texas.

[4] Nestler, D. E., "Compressible Turbulent Boundary Layer Heat Transfer to Rough Surfaces," AIAA Paper 70-742, Los Angeles, Calif., 1970.

[5] Strass, H. K. and Tyner, T. W., "Some Effects of Roughness on Stagnation-Point Heat Transfer at a Mach Number of 2, a Stagnation Temperature of 3,530°F, and a Reynolds Number of 2.5×10^6 per Foot," RM L58C10, May 1958, NACA.

[6] Diaconis, N. S., Wisniewski, R. J., and Jack, J. R., "Heat Transfer and Boundary-Layer Transition on Two Blunt Bodies at Mach Number 3.12," TN 4099, Oct. 1957, NACA.

[7] Dunavant, J. and Stone, H. W., "Effect of Roughness on Heat Transfer to Hemisphere Cylinders at Mach Numbers 10.4 and 11.4," TN D-3871, 1967, NASA.

[8] Persh, J., "A Procedure for Calculating the Boundary Layer Development in the Region of Transition from Laminar to Turbulent Flow," NAVORD Rept. 4438, March 1957, U. S. Naval Ordnance Lab., White Oak, Md.

[9] Cresci, R. J., MacKenzie, D. A., and Libby, P. A., "An Investigation of Laminar, Transitional, and Turbulent Heat Transfer on Blunt-Nosed Bodies in Hypersonic Flow," *Journal of the Aerospace Sciences*, Vol. 27, No. 6, June 1960, pp. 401–414.

[10] Laganelli, A. L. and Nestler, D. E., "Surface Ablation Pattern: A Phenomenology Study," *AIAA Journal*, Vol. 7, No. 7, July 1969, pp. 1319–1325.

[11] Dipprey, D. F. and Sabersky, R. H., "Heat and Momentum Transfer in Smooth and Rough Tubes at Various Prandtl Numbers," *International Journal of Heat and Mass Transfer*, Vol. 6, No. 5, May 1963, pp. 329–353.

[12] Thyson, N., Neuringer, J., Pallone, A., and Chen, K. K., "Nose Tip Shape Change Predictions During Atmospheric Reentry," AIAA Paper 70-827, Los Angeles, Calif., 1970.

An Experimental Investigation of Superheated Subliming Solid Thruster Performance

W. L. Owens Jr.*

Lockheed Missiles & Space Company, Sunnyvale, Calif.

Introduction

A LIMITATION of subliming solid thrusters has been the relatively low specific impulse obtained at propellant temperatures on the order of 100°F.[1] This Note presents experimental data for a superheated subliming solid thruster which indicate that a considerable improvement in performance is possible through an increase in gas temperature and an attendant reduction in molecular weight. The technology of vapor superheaters has advanced through its application to nitrogen, ammonia, and hydrogen resistojet systems.[2–5] Resistojets are available that will maintain an operating temperature of 1500°F with a heat loss of 12 w (Ref. 4) or 3700°F with a heat loss of ~30 w (Ref. 5). The experimental data presented show that delivered specific impulse (I_{sp}) for ammonium carbamate can be suitably predicted using a correlation for nozzle performance that has been shown to correlate most of the available data for throat Reynolds number (Re^*) in the range of 100–10,000. Total propulsion system mass as a function of total impulse for two gas temperatures and several thrust levels is shown using predicted I_{sp}'s.

Propellant Selection

Most candidate "subliming" solid propellants are ammonium salts which decompose to produce two–four vapor-phase molecules for every solid-phase molecule. Heating the "sublimed" vapor sufficiently causes the NH_3 to dissociate into N_2 and H_2 with an attendant improvement in specific impulse at the expense of the heat of dissociation.

Elimination of the ammonium salts that are toxic, explosive, undergo pyrolysis, or have too low a vapor pressure leaves essentially seven candidate substances: ammonium bicarbonate, -bisulfide, -bisulphite, -carbamate, -carbonate, -sulphide, and -sulphite. Ammonium carbamate was chosen from these because of its low dissociated molecular weight (26 at 100°F, 15.6 at 2000°F), suitable vapor pressure (210 torr at 100°F), and ease of manufacture. The nonelementary sublimation and dissociation reactions for ammonium carbamate ($NH_4CO_2NH_2$) are

$$NH_4CO_2NH_2 \overset{\text{Sub}}{\rightleftharpoons} CO_2 + 2\,NH_3, \quad CO_2 + 2(1 - \epsilon)NH_3 \overset{\text{Dissoc}}{\rightleftharpoons} CO_2 + \epsilon N_2 + 3\epsilon H_2$$

Presented as Paper 70-210 at the AIAA 8th Aerospace Sciences Meeting, New York, January 19–21, 1970; submitted October 13, 1970; revision received April 1, 1971.

* Staff Engineer, Propulsion Systems Department, Space Systems Division.